

Techniques for Correction of Atmospheric Artifacts in Sentinel 2 Images

¹Mr. D. Suresh Babu, ²Pampani Venkata Lakshmi Durga Keerthi, ³G. Snehitha

^{1,2,3}Velagapudi Ramakrishna Siddhartha Engineering College, Andhra Pradesh, India

¹dasarisuresh@vrsiddhartha.ac.in, ²pvldeerthi@gmail.com, ³snehithaguntaka09@gmail.com

Abstract : Remote sensing imagery is of utmost importance for overseeing alterations in the environment, assisting in the preservation of natural resources, and deepening our comprehension of worldwide carbon budgets and the consequences of climate change. However, these images are susceptible to various artifacts that can impact their quality and interpretation. One such artifact is sun glint, which refers to the reflection of light from water surfaces and poses a significant challenge when remotely sensing water column properties. The presence of atmospheric artifacts in remote sensing images can greatly influence the quality of the data and the resulting analysis. This project focuses on investigating two techniques, namely the Cox-Munk and Hedley methods, for effectively correcting these artifacts. These methods are employed to rectify surface reflectance and obtain precise information about the underlying features. The study also involves an analysis that compares these methods to evaluate their efficiency in rectifying atmospheric artifacts in remote sensing images. Real-life remote sensing data is utilized to demonstrate the implementation of these techniques, and a comprehensive analysis is conducted on the obtained results. The findings of this study can provide valuable insights for researchers and professionals working with remote sensing data, particularly those involved in atmospheric correction and image processing.

Keywords—Remote Sensing Images, atmospheric artifacts, sun glint, correction,Cox-Munk and Hedley techniques.

I. INTRODUCTION

Ocean and coastal remote sensing plays a crucial role in monitoring environmental changes, facilitating resource conservation, and understanding the impacts of climate change and the global carbon budget. However, the presence of glint in images often poses challenges and affects the accuracy of various image processing techniques. Sun glint is a intricate phenomenon that limits the quantity and precision of the remotely acquired data from aquatic environments. It encompasses the upper boundary of the air-water interface reflecting sunlight in a specular manner. It affects various types of marine imagery, making it difficult to accurately retrieve information from beneath the water surface. Sun glint manifests in images when the water surface aligns in a way that directs sunlight straight towards the sensor, and its occurrence is influenced by factors like the condition of the sea surface, the sun's position, and the viewing angle. The specular reflection of light from the water surface significantly affects the radiance received by the sensor, making it challenging to retrieve data on parameters like benthic characteristics, chlorophyll content,

or bathymetry. Overcoming this challenge requires a robust algorithm capable of effectively isolating and mitigating the impact of glare while maintaining high measurement

1.1 Atmospheric artifacts

Atmospheric artifacts are visual anomalies that can appear in images or videos due to atmospheric conditions. These artifacts can distort the quality of the image or video and affect the sharpness, contrast, and color balance.

1.2 Sun Glint

In Level 1 imagery, sun glint[1] in true color images is observed as a prominent white strip. This phenomenon arises from the reflection of sunlight on the ocean's surface. The reflected sunlight's intensity far exceeds the light from beneath the water, making it exceptionally difficult, and sometimes infeasible, to obtain precise data on in-water constituents through direct measurements. In Figures 1(a) and 1(b), illustrate the scene both prior to and after calculating and subtracting the sun glint effects from the visible bands[2].

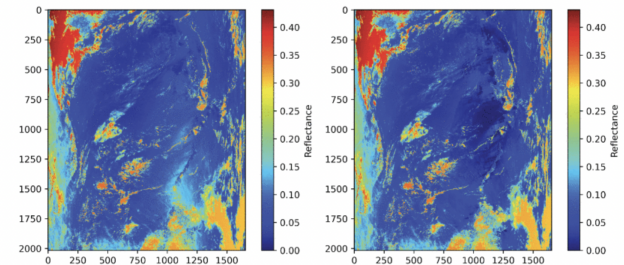


Figure 1(a)

Figure 1(b)

1.3 Water leaving radiance

It is of utmost importance in ocean color remote sensing since it denotes the radiance emitted from the sea surface, which then propagates upward into the atmosphere. It serves as a crucial parameter as its spectral characteristics provide valuable information about the properties of the sea-surface layer, including the concentration of chlorophyll-a.

1.4 NIR radiance

The amount of electromagnetic radiation in the near infrared region of the electromagnetic spectrum that an object emits or reflects is referred to as near-infrared (NIR) radiance[12]. NIR radiation is frequently used in numerous applications, including imaging, spectroscopy, and remote sensing, and has a wavelength range of roughly 700 to 2500 nanometers. It is typically expressed in radiance or radiant intensity units

and can be used to determine an object's reflectance characteristics.

1.5 MOTIVATION

Effective techniques for correcting artifacts in remote sensing images are crucial for enhancing data quality and reliability. This is vital in various fields, including monitoring of ocean color, studying underwater ecosystems, environmental monitoring, disaster response, and urban planning, where accurate remote sensing data can aid decision-making. Furthermore, the development of these techniques can lead to advancements in remote sensing and signal processing, enabling more comprehensive data collection in the future.

1.6 PROBLEM STATEMENT

Atmospheric artifacts in Sentinel-2 images can degrade the quality of the data and make it difficult to extract accurate information. The aim of this study is to implement the techniques for correcting these artifacts, in order to improve the quality and usability of Sentinel-2 data for various applications.

1.7 OBJECTIVES

The following points outline the main objectives of this project:

- To get an idea about different atmospheric correction algorithms.
- To implement Cox and munk and Hedley techniques to correct the sun glint present in remote sensing images.

1.8 ADVANTAGES

- Improved accuracy: Correcting for atmospheric effects reduces errors and uncertainties in the data, allowing for more accurate analysis and interpretation.
- Quantitative analysis: Atmospheric correction enables quantitative analysis, such as the measurement of surface reflectance, vegetation indices, and other biophysical parameters, which is essential for scientific research and monitoring.
- Data interoperability: Corrected satellite images are more compatible with data from other sources, such as ground-based measurements, climate data, and other satellite imagery, facilitating integration and fusion of different datasets

1.9 APPLICATIONS

- Oceanography: Remote sensing images help oceanographers understand physical properties of oceans such as temperature, currents, and sea surface height.
- Coastal zone management: Remote sensing images can map shoreline changes, detect harmful algal blooms, and identify oil spills for effective coastal zone management.

- Water quality assessment: Remote sensing images provide data on water body optical properties such as suspended sediment, chlorophyll concentration, and turbidity for water quality assessment and pollution detection.
- Flood and drought monitoring: Remote sensing images help monitor and identify the extent and severity of floods and droughts to coordinate relief efforts.
- Fisheries management: Remote sensing images detect phytoplankton blooms, identify fish spawning grounds, and track fish population movements for efficient fisheries management.

1.12 ORGANIZATION

The paper's organization is as follows: Section 1 offers a review of the literature on artifact correction and classification, Section 2 details about the requirements, Section 3 details the proposed system methodology and the architecture, and Section 4 delves into the results and discussion and then Section 5 concludes the paper.

I.RELATED WORKS

The automated methodology discussed in the paper [3] is designed to enhance the efficiency of correcting high-spatial-resolution (HSR) satellite images. This approach leverages atmospheric aerosol data from geostationary satellites to align Aerosol Optical Depth (AOD) with HSR image attributes, simplifying atmospheric correction and precise surface reflectance (SR) estimation. One notable advantage is the complete automation of the process, reducing manual intervention and saving time and effort. This method effectively addresses the challenging task of HSR image correction and circumvents obstacles related to acquiring accurate AOD data. However, its applicability is contingent on the availability and accuracy of geostationary aerosol data, and the spatial and temporal resolution matching between aerosol data and HSR images, limiting its generalizability.

The investigation focuses on the methodology detailed in reference [4], highlighting the Glint Removal through Contrast Minimization (GRCM) technique, which offers a quantitative and efficient solution for eliminating sun glint interference from top-of-atmosphere (TOA) reflectances in the visible and near-infrared wavelengths. GRCM leverages shortwave infrared observations of sun glint's structure to isolate and eliminate its impact, demanding high spatial resolution imagery within a 10-50 meter range to accurately capture sun glint features and meet specific criteria for radiometric resolution, signal-to-noise ratio, and temporal synchronization between band acquisitions. Key advantages encompass the elimination of the need for additional sea surface roughness data and the effective handling of thin clouds and sun glint, expanding data coverage. However, the method does mandate high spatial resolution imagery and adherence to the specified criteria.

In study [5], the SAAC-Net, an innovative end-to-end deep neural network (DNN) model, is introduced, offering a novel approach by directly predicting surface reflectance from top-of-atmosphere (TOA) images, bypassing the reliance on atmospheric variables, including Aerosol Optical Depth (AOD), humidity, and barometric pressure. The

development and training of this model utilized TOA and bottom of atmosphere (BOA) pairs generated by the LaSRC algorithm, which is grounded in a physics-based framework. Evaluation of the predicted surface reflectance drew upon Landsat 8 data and on-site measurements obtained from RadCalNet. Notably, the study addressed seasonal and spatial variability but did not encompass long-term temporal variability in TOA and BOA values. SAAC-Net's advantages lie in its ability to predict surface reflectance directly from TOA imagery, eliminating the need for atmospheric parameter input, while its limitation lies in the omission of accounting for long-term temporal variability in TOA and BOA values, potentially affecting its performance over extended image acquisition periods.

In a recent study [6], researchers developed an algorithm for estimating water leaving reflectance in murky coastal waters using spectrum matching. They utilized shortwave IR (SWIR) bands, specifically the 1.24, 1.61, and 2.25 micrometer bands in the VIIRS sensor, to estimate aerosol models and optical depths. This information was then extended to the visible spectrum for calculating water leaving flux. While this approach offers advantages, such as improved accuracy and wider spatial coverage, it does rely on SWIR bands, which may not be available in all sensors, and it can be computationally intensive, potentially limiting its scalability for large-scale data processing.

In [7], an innovative technique leverages a deep learning algorithm to identify and categorize sun glint in high-resolution aerial images captured above shallow marine regions. This algorithm, based on CNN that is trained on diverse environmental conditions, exhibits impressive accuracy in detecting sun glint. This approach holds promise for refining remote sensing data in shallow marine environment monitoring but lacks correction capabilities and might benefit from comparison with existing methods for further enhancements.

In the methodology outlined in [8], a novel approach is employed, centered on noise de-correlation. This method effectively segregates the sun glint signal from the surrounding image by utilizing a noise correlation matrix. This matrix is constructed through an analysis of the image's statistical characteristics, facilitating the estimation of the correlation between the sun glint and the image's noise. To showcase the efficacy of this technique, the researchers put it to the test with a Landsat 8 image of a coastal region and compared the outcomes to those generated by two widely used sun glint correction methods. Notably, their method exhibited superior accuracy in contrast to the 6S method and the MUMM algorithm. However, it's worth noting that the study's reliance on just one Landsat 8 image for evaluation may restrict the broader applicability of their findings.

In [9], the innovative Dark Spectrum Fitting (DSF) technique uses dark targets within a subscene to create a "dark spectrum" for estimating atmospheric path reflectance with the most suitable aerosol model. This automated method is highly versatile, exemplified in a North Sea study. DSF also estimates sun glint-induced reflectance with SWIR bands and corrects it, greatly improving data quality for nadir viewing sensors. Its key advantages include open-source availability, versatile applications, and precise atmospheric correction.

The methodology outlined in [10] introduces QUAC (Quick Atmospheric Correction), a specialized atmospheric correction method tailored for the VNIR-SWIR range, spanning both multi- and hyperspectral imagery. This approach employs an in-scene method, directly deriving parameters for atmospheric compensation from the pixel spectra within the scene. It is rooted in the empirical observation that the mean spectrum of various material spectra holds valuable information. QUAC is notable for its capability to obtain reasonably precise reflectance spectra, even in cases where the sensor lacks the necessary radiometric or wavelength calibration, or when the intensity of solar illumination is uncertain. The efficacy of QUAC is evident in its successful application for atmospheric correction in AVIRIS and HyMap datasets, offering the advantages of significantly faster computational speed and approximate results. It's compatible with any collection of VNIR-SWIR bands, making it suitable for both multispectral and hyperspectral sensors, though it is limited to VNIR-SWIR spectral imagery.

Addressing the issue of specular reflection of solar radiation on uneven water surfaces has posed a notable challenge in shallow-water remote sensing[14]. Recently, Hochberg et al. introduced an efficient solution to reduce the influence of 'sun glint' in images acquired through remote sensing, the method leverages the brightness from a near-infrared (NIR) band. Their technique enhanced the precision of the classification of benthic habitats. However, as described, the approach displayed sensitivity to outlier pixels and required the laborious process of masking land and cloud regions that consumes a significant amount of time. and lacked a user-friendly implementation format. In response, they offered an improved, robust version of this method, eliminates the need for masking, and is exceptionally straightforward to implement. They anticipated that this practical approach will facilitate the widespread acceptance and implementation of this technique, which is efficient and easy to use, among the community of experts in remote sensing in aquatic environments..

II. REQUIREMENTS

2.1 SOFTWARE REQUIREMENTS

- OS: Windows 10 or higher(64-bit) MacOS 12.6 or higher
- Programming language: Python 3.9
- Python libraries: Skicit-learn, PySimpleGUI , pandas, numpy
- IDE : Visual Studio code or an interactive web based platform like Jupyter Notebook

2.2 HARDWARE REQUIREMENTS

- RAM: 4GB or higher
- Processor: i3 or above, is preferred.
- GPU: 12 GB

III METHODS

This section outlines the system's architecture, the implementation methodology, and the dataset used.

3.1 Architecture

Figure 2 displays the system model for correcting sun glint. The system operates as follows: upon data collection, the dataset is initially preprocessed by addressing missing values. The missing values were filled using mean or median imputation techniques. Median imputation involves replacing missing values in a variable with the median of the available values in that variable. Apply masking to obtain the visible bands instead of working with all the 13 bands.

Once the user selects either the correcting technique proposed by Hedley et al. or the method by Cox and Munk, the chosen technique is applied to the preprocessed data. This involves implementing the specific algorithm or approach associated with the selected technique.

After the correction is applied, the performance of the technique is evaluated using two commonly used metrics: Mean Absolute Error (MAE) and the Root Mean Squared Error (RMSE). These metrics provide a quantitative assessment of the corrected data and help compare the effectiveness of the chosen technique to improve the data quality.

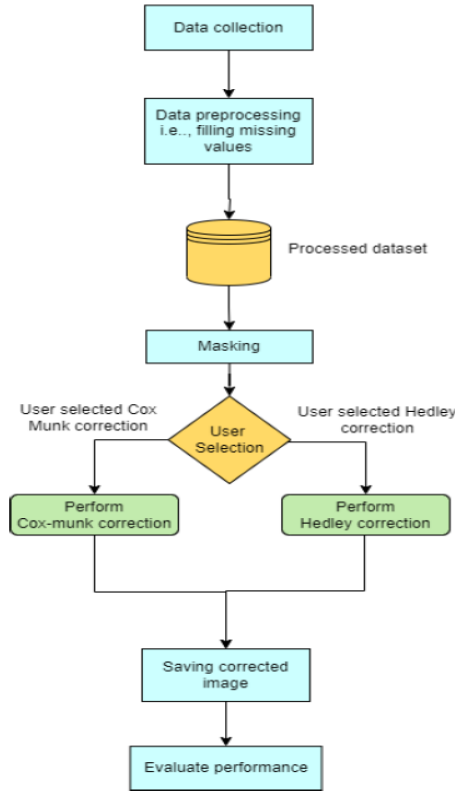


Figure 2: Proposed System Model of the Application

3.2 Methodology

This section delves into the various modules incorporated within the project. The included modules are as follows: Data collection and preprocessing the data, Applying the method of Hedley et al., Applying the method of Cox and Munk, Evaluating the performance of both the techniques.

3.2.1 Preprocessing

Collecting the dataset which contains manually extracted data by visual observed 30 Satellite images of Sentinel 2 level 1C. Preprocessing the data by filling in the missing values. The missing values were filled using mean or median

imputation techniques. Median imputation involves replacing missing values in a variable with the median of the available values in that variable.

$$\begin{aligned} \text{Med}(X) &= X[\frac{n+1}{2}] && \text{if } n \text{ is odd} \\ &= \frac{X[\frac{n}{2}]+X[\frac{n+1}{2}]}{2} && \text{if } n \text{ is even} \end{aligned} \quad (1)$$

After sorting the non-missing values in ascending order, find the median using (1), then replace missing values with the median obtained.

3.2.2 Applying the method of Hedley et al.

The proposed approach adjusts the correlation in the interplay of the NIR signal and the sun glint by leveraging one or more image regions. These areas were chosen so that they would have a variety of pixel glint levels, but they also have very low levels of radiance in the NIR spectrum, particularly in deep water regions, and an assumed constant underlying brightness. Using all the pixels in the chosen regions, a linear regression is created for each band between the NIR radiance and the radiance of the specific band.

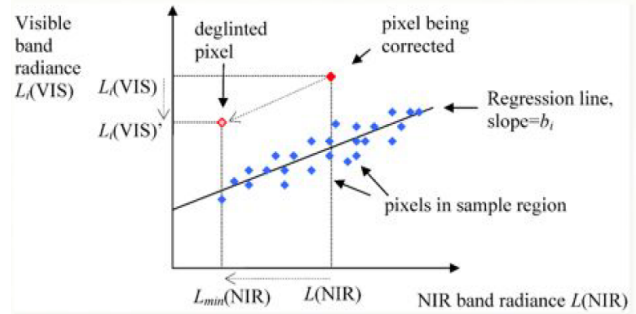


Figure 3: The graphical depiction of Hedley et al.'s glint correction method[15]

The radiance corrected in i th band is expressed as follows:

$$L_i(VIS) = L_i(VIS) - b_i [L(NIR) - L_{min}(NIR)] \quad (2)$$

3.2.3 Applying the method of Cox and Munk:

Cox and Munk (1954a and 1954b) conducted research focusing on aerial photographs that captured the patterns of solar glitter on wind-rippled sea surfaces. These photographs allowed them to extract valuable information about the statistical properties of the sea surface slope, correlating them with varying wind speeds. A specific example can be seen in Figure 4. The measured wind speed in the photographed area, obtained from a ship, was 4.6 m/s. It is worth noting the related work by Cox and Munk (1955) for further insights. Under conditions where wind speed and swell are not present, resulting in a completely flat surface, and with a dark sky, the glimmering pattern will manifest as a solitary intense point, positioned precisely at the photograph's center, it aligns perfectly with the direction of the Sun's gleaming reflection.

Nevertheless, when wind is present, the ocean's surface becomes agitated, resulting in the Sun's direct beam reflecting over a larger expanse of the water's surface and dispersing toward the viewer. To reflect a solar ray in the viewer's direction, a wave facet must be angled in a specific way, allowing the incoming Sun's ray to redirect toward the

observer. This concept is effectively demonstrated in Figure 5.

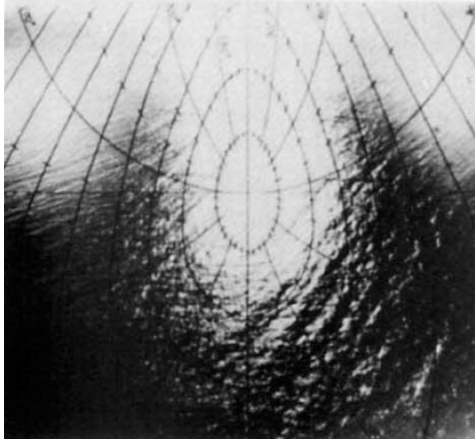


Figure 4: This image showcases a glistening pattern that signifies a wind speed of 4.6 meters per second recorded at an altitude of 610 meters (2,000 feet). The view is azimuthal, directly facing the Sun, and angled downwards towards the sea surface. The central bright area represents the Sun's glitter pattern, while the upper left and right sections exhibit glints, likely originating from the background sky or possibly from clouds.[15]

The tilted wave facet, depicted as the blue triangle, is responsible for reflecting an incident solar ray, denoted as ξ' , in the direction of the observer, ξ . The coordinate system $(\hat{x}, \hat{y}, \hat{z})$, denoted by the arrows in green, is centered around the Sun. The $-\hat{x}$ cap points horizontally in the direction of the Sun, \hat{z} points directly upward (perpendicular to the average sea surface), and \hat{y} is determined as the result of the cross product between \hat{z} and \hat{x} . The unit vector \hat{n} signifies the normal to the inclined facet. The facet's tilt concerning the normal of the average sea surface is quantified by the polar angle $\beta = \cos^{-1}(\hat{n} \times \hat{z})$. Additionally, the azimuthal angle, α , gauges the facet's orientation concerning the \hat{x} axis, with α being assessed in a clockwise fashion starting from \hat{x} as depicted.

Investigating the statistical attributes of sea surface slopes in relation to wind speed, researchers conducted a study using aerial images of the Sun's glimmer patterns on turbulent ocean surfaces, as detailed in reference [15]. Expanding on the pioneering work of Cox and Munk, the statistical distribution of sea surface slopes, identified as n_a and n_c , can be approximated as a bivariate Gaussian distribution, providing a rough representation of their characteristics.

$$\rho(n_a, n_c) = \frac{1}{2\pi\sigma_a\sigma_c} \exp\left[-\frac{1}{2}\left(\frac{n_a^2}{\sigma_a^2} + \frac{n_c^2}{\sigma_c^2}\right)\right] \quad (3)$$

Figure 7: The statistical pattern of sea surface slope variations that occur randomly.

Where σ_a^2 and σ_c^2 are the variances of the slopes in the along wind and crosswind directions.

Calculate the slope correlation length using the Cox and Munk model .

$$L = 0.74 \lambda / (0.22U + 0.333\lambda) \quad (4)$$

Convert slope variance and correlation length to roughness parameters. Apply the roughness correction to the measured signals and output the corrected signals

3.2.4 Evaluating the performance of both the techniques..

Finally, the accuracy of the atmospheric correction can be evaluated by comparing the corrected data to the ground truth data using Mean Absolute Error(MAE) and Root Mean Square Error(RMSE).

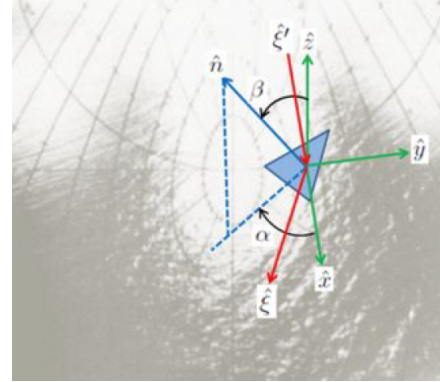


Figure 5: Illustration depicting a tilted wave facet (represented by a blue triangle) reflecting an incoming solar ray towards an observer's direction[15]

3.3 Dataset Collection:

The dataset[11] used in this study was obtained from Figshare, an openly accessible online repository. It includes a large number of water spectra extracted from 30 Sentinel 2 satellite images. These spectra were manually retrieved from regions of deep water characterized by significant noise and the presence of sunglint. The images were collected over multiple years, with varying numbers of images in each year. The images consist of different bands with varying spatial resolutions. To maintain consistency, the bands with different spatial resolutions were resampled before extracting the spectra. The obtained spectral data is archived in .csv files, which are labeled with the respective Sentinel 2 product names.

3.4 Algorithm:

The model's algorithm is outlined as follows:

Input: Dataset of 30 csv files collected from Sentinel 2 satellite which require correction of one of the artifacts - Sun glint.[11]

Output: Sunglint corrected image using the selected technique.

Process:

Step 1: The dataset from the Sentinel-2 satellite, which includes sunglint, is gathered from the Figshare website.

Step 2: Initial data preprocessing

step 2.1: Fill missing values using median imputation method.

$$Med(X) = \begin{cases} X[\frac{n+1}{2}] & \text{if } n \text{ is odd} \\ \frac{X[\frac{n}{2}] + X[\frac{n+1}{2}]}{2} & \text{if } n \text{ is even} \end{cases} \quad (1)$$

step 2.2: Apply masking to obtain the visible bands instead of working with all the 13 bands.

Step 3: Method of Hedley

step 3.1: Now , the above preprocessed image undergoes Hedley correction of atmospheric artifacts, by applying (2) to correct radiance at ith band.

Step 4: Method of Cox - Munk

step 4.1: If the chosen method is to correct radiance values using Cox - Munk method, the method considers the sea surface slope characteristics. Cox and Munk determined that the statistical distribution of stochastic slopes of sea surface, represented by η_a and η_c , can be well approximated by a bivariate Gaussian distribution.

$$\rho(\eta_a, \eta_c) = \frac{1}{2\pi\sigma_a\sigma_c} \exp\left[-\frac{1}{2}\left(\frac{\eta_a^2}{\sigma_a^2} + \frac{\eta_c^2}{\sigma_c^2}\right)\right]$$

where σ_a^2 and σ_c^2 are the variances of the slopes in the along-wind and crosswind directions.

step 4.2: Calculate the slope correlation length using the Cox and Munk model using (4).

Step 4.3: Convert slope variance and correlation length to roughness parameters.

Step 4.4: Apply the roughness correction to the measured signals and output the corrected signals.

Step 5: Compile the model

Step 6: Evaluating the performance of both the techniques.

Step 6.1: The accuracy of the atmospheric correction can be evaluated by comparing the corrected data to the ground truth data using Mean Absolute Error(MAE).

$$MAE = (1/n) * \sum_{i=1}^n |Y_i - \hat{Y}_i| \quad (5)$$

where n represents the total number of data points, Y_i represents the actual value, \hat{Y}_i is the predicted value, Σ denotes the summation operator, summing the absolute differences for all data points

Step 6.2: the accuracy of the atmospheric correction can be evaluated by comparing the corrected data to ground truth data using Root Mean Square Error(RMSE).

$$RMSE = \sqrt{(1/n * \sum (y_i - \hat{y}_i)^2)} \quad (6)$$

where n refers to the total number of observations or data points, y_i is the true value of the data point at index 'i', \hat{y}_i represents the predicted the value associated with the data point at index 'i', the symbol Σ signifies the summation operation, implying that you should add together the squared variances across all data points.

Step 7: Obtained sunglint corrected images .

IV RESULTS AND DISCUSSION

The overall complete idea of this project is to find out the techniques for correction of an atmospheric artifact i.e, sunglint in remote sensing images. This project includes collection of a dataset containing Sentinel2 images with sunglint. It is a collection of files with .csv extension which contains Lat,lon and 13 band radiance values as attributes. The collected dataset is preprocessed for filling the missing values using median imputation method. We then explained the Hedley and Cox and Munk techniques for the correction of sunglint . After implementing the two techniques, they are tested using the metrics - MAE and RMSE. In Figure 8a and 8b, you'll find the graphical user interface (GUI) of the project. This interface enables users to provide input, prompts them to select from a range of available methods, and then prompts them to submit their choice. Once the selection is made, the system proceeds to save the corrected file and subsequently displays the file's path for the user's reference.

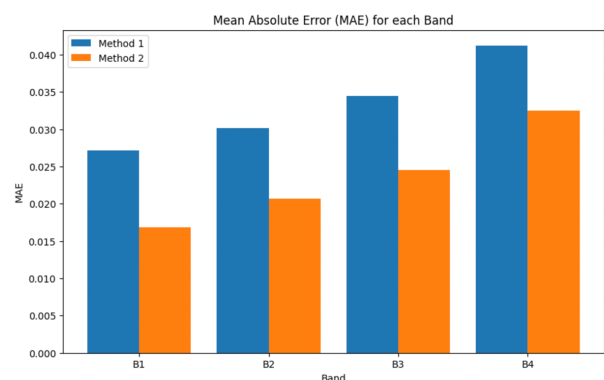


Figure 6: Performance Analysis using MAE

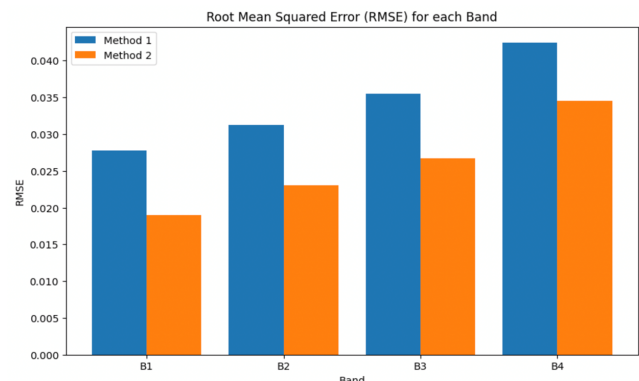


Figure 7: Performance Analysis using RMSE

The above Figures 6, 7 depicts the MAE and RMSE graphs plotted for both the methods - Hedley(method1) and Cox and Munk(method2) respectively.

V CONCLUSION

The project focused on developing techniques for correcting atmospheric artifacts, specifically sun glint, in Sentinel-2 images to improve their quality and usability. We successfully implemented a correction technique for sun glint,which involved estimating and removing the reflection of sunlight on the water's surface in the images.



Figure 8a: GUI of the implemented project



Figure 8b: GUI of the implemented project

In the future, we aim to expand our work to correct radiometric artifacts as well, which can also affect the quality of Sentinel-2 data. Radiometric artifacts can include striping, banding, and sensor noise, among others.

In addition to these technical developments, we also plan to implement these processing technique in various applications like Land cover classification, oceanography, and coastal monitoring.

REFERENCES

- [1] X. Wu, Y. Lu, J. Jiao, J. Ding, W. Fu and W. Qian, "Using Sea Wave Simulations to Interpret the Sunglint Reflection Variation With Different Spatial Resolutions," in IEEE Geoscience and Remote Sensing Letters, vol. 19, pp. 1-4, 2022, Art no. 1501304, doi: 10.1109/LGRS.2020.3033700.
- [2] N. Li, L. Guan and H. Gao, "Sun Glint Correction Based on BRDF Model for Improving the HY-1C/COCTS Clear-Sky Coverage," in IEEE Geoscience and Remote Sensing Letters, vol. 20, pp. 1-5, 2023, Art no. 1500205, doi: 10.1109/LGRS.2022.3231010.
- [3] Liu, S.; Zhang, Y.; Zhao, L.; Chen, X.; Zhou, R.; Zheng, F.; Li, Z.; Li, J.; Yang, H.; Li, H.; Yang, J.; Gao, H.; Gu, X. QUantitative and Automatic AtmosphericCorrection (QUAAC): Application and Validation.Sensors2022,22,3280.https://doi.org/10.3390/s22093280
- [4] Soppa, M.A.; Silva, B.; Steinmetz, F.; Keith, D.; Scheffler, D.; Bohn, N.; Bracher, A. Assessment of Polymer Atmospheric Correction Algorithm for Hyperspectral Remote Sensing Imagery over CoastalWaters. Sensors 2021, 21, 4125. https://doi.org/10.3390/s21124125
- [5] Shah, Maitrik; Raval, Mehul (2022): A DEEP

LEARNING MODEL FOR ATMOSPHERIC CORRECTION OF SATELLITE IMAGES. TechRxiv. Preprint.https://doi.org/10.36227/techrxiv.21787166.v1

- [6] Gao, B.-C.; Li, R.-R. A Multi-Band Atmospheric Correction Algorithm for Deriving Water Leaving Reflectances over Turbid Waters from VIIRS Data. *Remote Sens.* 2023, 15, 425. https://doi.org/10.3390/rs15020425.
- [7] Giles, A., Davies, J., Ren, K., & Kelaher, B. P. (2021). A deep learning algorithm to detect and classify sun glint from high-resolution aerial imagery over shallow marine environments. *Isprs Journal of Photogrammetry and Remote Sensing*, 181, 20–26. https://doi.org/10.1016/j.isprsjprs.2021.09.004
- [8] Cui, A., Zhang, J., Ma, Y., & Zhang, X. (2022). A Noise De-Correlation based sun glint correction method and its effect on shallow bathymetry inversion. *Remote Sensing*, 14(23), 5981. https://doi.org/10.3390/rs14235981
- [9] Vanhellemont, Q. (2019). Adaptation of the dark spectrum fitting atmospheric correction for aquatic applications of the Landsat and Sentinel-2 archives. *Remote Sensing of Environment*, 225, 175–192. https://doi.org/10.1016/j.rse.2019.03.010
- [10] L. S. Bernstein, S. M. Adler-Golden, X. Jin, B. Gregor and R. L. Sundberg, "Quick atmospheric correction (QUAC) code for VNIR-SWIR spectral imagery: Algorithm details," 2012 4th Workshop on Hyperspectral Image and Signal Processing: Evolution in Remote Sensing (WHISPERS), Shanghai, China, 2012, pp. 1-4, doi: 10.1109/WHISPERS.2012.6874311.
- [11] Kristollari, Viktoria; Karathassi, Vassilia (2020): Sentinel 2 manually extracted deep water spectra with high noise levels and sunglint. figshare. Dataset. https://doi.org/10.6084/m9.figshare.8075396.v1
- [12] E. Takada, Y. Hosono, T. Kakuta, M. Yamazaki, H. Takahashi and M. Nakazawa, "Application of red and near infrared emission from rare earth ions for radiation measurements based on optical fibers," in IEEE Transactions on Nuclear Science, vol. 45, no. 3, pp. 556-560, June 1998, doi: 10.1109/23.682447.
- [13] Kay S, Hedley JD, Lavender S. Sun Glint Correction of High and Low Spatial Resolution Images of Aquatic Scenes: a Review of Methods for Visible and Near-Infrared Wavelengths. *Remote Sensing*. 2009; 1(4):697-730. https://doi.org/10.3390/rs1040697
- [14] Hedley, John & Harborne, Alastair & Mumby, Peter. (2005). Technical note: Simple and robust removal of sun glint for mapping shallow-water benthos. *International Journal of Remote Sensing - INT J REMOTE SENS.* 26. 2107-2112. 10.1080/01431160500034086.
- [15] https://oceanopticsbook.info/view/surfaces/cox-munk-sea-surface-slope-statistics